Thermal-vibrational amplitudes of silicon determined by channeling-radiation measurements

J. O. Kephart
IBM Thomas J. Watson Research Center, Yorktown Heights, New York 10598

B. L. Berman
Department of Physics, The George Washington University, Washington, D.C. 20052

R. H. Pantell
Department of Electrical Engineering, Stanford University, Stanford, California 94305

S. Datz
Physics Division, Oak Ridge National Laboratory, Oak Ridge, Tennessee 37831

R. K. Klein
Advanced Micro Devices, Inc., Sunnyvale, California 94088

H. Park
AT&T Bell Laboratories, Murray Hill, New Jersey 07974
(Received 19 December 1990)

We have observed radiation emitted by electrons channeled along the (110) and (100) planes of silicon for four different beam energies ranging from 16.9 to 54.5 MeV. Taking advantage of the great sensitivity of the positions of some of the spectral peaks to the vibrations of the Si nuclei, we have determined the vibrational amplitude at room temperature to be 0.0813 ± 0.0009 Å for the (110) plane and 0.0789 ± 0.0007 Å for the (100) plane. The values obtained from channeling-radiation measurements differ substantially from the value of 0.075 Å obtained from x-ray-diffraction measurements, which fail to distinguish between vibrational amplitudes for different planes. For many crystals, electron-channeling-radiation measurements of thermal-vibrational amplitudes may prove to be more accurate than x-ray measurements.

I. INTRODUCTION

In a number of previous papers, we have reported measurements of channeling radiation (CR) which have thrown light on properties of both perfect and imperfect crystals; Refs. 1–4 review our work in this field. In particular, Ref. 5 details our use of the interplanar potentials derived from isolated-atomic potentials to interpret our channeling-radiation studies with perfect diamond crystals, Refs. 6 and 7 report our determination of the Debye temperature for silicon from measurements of channeling radiation from cooled crystals, and Ref. 8 reports the determination of occupation lengths in silicon crystals. In the present work we extend the use of the continuum-potential approximation to a systematic study of channeling radiation from silicon at several incident electron-beam energies in order to determine the thermal-vibrational amplitudes for both the (110) and (100) planes at room temperature.

The experimental method is detailed in Refs. 1 and 3. Briefly, a well-collimated, low-divergence beam of electrons from the Lawrence Livermore National Laboratory Electron-Positron Linear Accelerator is incident on the crystal under study, which is mounted in a three-axis goniometer. After having passed through the crystal, the electron beam is swept by a magnet into a deep beam dump. The zero-degree spectrum of channeling radiation produced in the crystal when one of its major planes is aligned along the beam direction is measured in a high-resolution germanium-lithium x-ray spectrometer. Details of the experimental apparatus and setup, beam-tuning procedures, etc., are given in Refs. 1, 3, and 5.

Many details of the data reduction and analysis are given in Refs. 5, 8, and 9. Over the years, our refinement of these procedures has kept pace with the improvement in quality of our experimental data. A secondary purpose of this paper is to present our most accurate measurements of channeling-radiation spectra of electrons channeled along the two major planes of silicon.

II. ANALYSIS

A. Preliminaries

In most respects, experimentally obtained electron planar channeling-radiation spectra are usually in good agreement with spectra calculated by the technique of Refs. 5 and 8. For example, Fig. 1 compares calculated and observed spectra for the case of 30.5-MeV ($\gamma=60.78$) electrons channeled along the (110) planes of a silicon crystal. The observed spectrum was obtained by the experimental procedures outlined above, and was processed by subtraction of the bremsstrahlung background and corrections for detector efficiency, escape of 9.8-keV

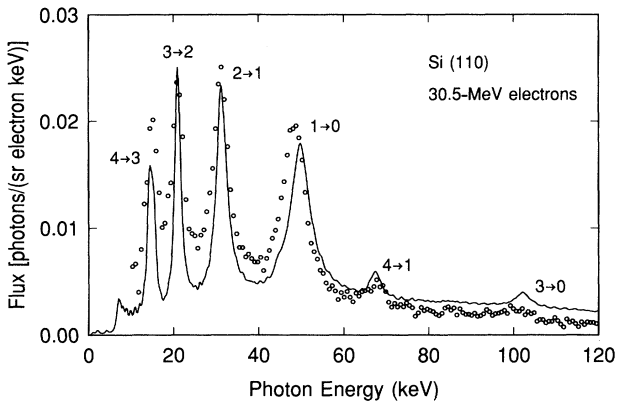

FIG. 1. Calculated (solid curve) and observed channeling-radiation spectra of 30.5-MeV electrons channeled along the (110) planes of silicon. Calculation assumes the nominal beam energy of $\gamma=60.78$ and vibrational amplitude $u=0.075$ Å. All except the $1\rightarrow0$ and $3\rightarrow0$ transitions match the observed spectrum to within experimental error.

x rays from the Ge detector, and pileup, as described in Ref. 9. Numerical values for the observed and calculated peak energies are given in Table I. It can be seen that the calculated positions of the peaks associated with the $4\rightarrow3$, $3\rightarrow2$, $2\rightarrow1$, and $4\rightarrow1$ transitions are in excellent agreement with the measured positions, but the calculated $1\rightarrow0$ and $3\rightarrow0$ energies are significantly too high.

There are two possible weak links in the chain of calculations that lead to the calculated curves in Fig. 1. The first of these occurs at the very beginning of the calculation, before the application of the continuum-potential approximation.[8,9] The crystal potential is computed by adding the potentials of isolated atoms. Might the covalent bonding of the silicon atoms in the crystal, which is not taken into account by this superposition, result in a shift of the calculated photon energies? A careful consideration of this question reveals that covalent bonding in silicon cannot be blamed for these discrepancies. Covalent bonding in diamond, which has the same structure as silicon, *does* cause a noticeable shift in photon energies for electrons channeling along the $\langle 110\rangle$ axis of the (111) plane,[5] but the geometry of the bond is such that the shift is negligible for the (100) and (111) planes.[2,5] Furthermore, covalent bonding has much less of an effect on the potential of silicon that it does for diamond because a smaller fraction of the electrons participate in the bond for silicon—4 out of 14 for silicon as opposed to 4 out of 6 for diamond. A quantitative comparison of a Si(110) potential obtained from a solid-state pseudopotential calculation[10] with a Si(110) potential obtained from the usual superposition of atomic potentials confirms that covalent bonding has a negligible effect on this plane.

TABLE I. Calculated and observed channeling-radiation peak energies for 30.5-MeV electrons channeled along the (110) planes of Si. The calculated energies are based upon the assumptions $\gamma=60.78$ and $u=0.075$ Å.

Transition	$E_{\gamma(\text{calc})}$ (keV)	$E_{\gamma(\text{obs})}$ (keV)
$(4\rightarrow3)_{(110)}$	14.76	14.9±0.2
$(3\rightarrow2)_{(110)}$	20.98	21.1±0.2
$(2\rightarrow1)_{(110)}$	31.22	31.1±0.2
$(1\rightarrow0)_{(110)}$	49.76	48.4±0.3
$(4\rightarrow1)_{(110)}$	67.33	66.8±0.5
$(3\rightarrow0)_{(110)}$	102.05	100.2±0.8

The second possible weak link in the calculations concerns the effect of multiple scattering on the positions of the observed CR peaks. Planar-channeled particles scatter in the direction parallel to the planes and perpendicular to the forward direction. A particle traveling in a direction θ with respect to the forward direction may emit channeling radiation in the forward direction. Since this radiation is emitted at an angle of $-\theta$ with respect to the particle's direction, the photon energy will be downshifted by a factor of approximately $(\theta\gamma)^2$, provided that $\theta\ll\gamma^{-1}$. As a result of the downward Doppler shift of radiation emitted by scattered particles, channeling-radiation peaks acquire a low-energy tail and the maxima are shifted slightly downward in energy. Could the downward shift induced by multiple scattering account for the discrepancies between the observed and calculated peak energies?

B. Multiple scattering

In order to investigate the influence of multiple scattering on channeling-radiation spectra, a computer program capable of simulating this effect was developed. Although little is known about the multiple scattering of planar-channeled particles, it is reasonable to assume that their behavior is qualitatively similar to that of unchanneled particles, which *is* reasonably well understood.[11–13] The one major difference is that the multiple scattering of planar-channeled particles is one dimensional rather than two dimensional—it is constrained to take place in the direction parallel to the planes and perpendicular to the forward direction. If the direction of the scattered particle with respect to the forward direction is denoted as $\Omega_e=(\theta_e,\phi_e)$, where ϕ_e is measured from the $\hat{\mathbf{x}}$ direction (the direction normal to the planes), then $\phi_e=90°$. Based on these considerations, we postulate that the multiple-scattering distribution for channeled particles in the state $|n,\kappa\rangle$ can be written in the form

$$f_{n,\kappa}(\theta_e;z)\approx\frac{1}{\sqrt{\pi}\Theta_{n,\kappa}(z)}e^{-\theta_e^2/\Theta_{n,\kappa}^2(z)}, \tag{1}$$

where

$$\Theta_{n,\kappa}(z)\approx A_{n,\kappa}z^{1/2} \tag{2}$$

is the multiple-scattering angle as a function of the penetration depth z. The proportionality constant A_{MS} is known for unchanneled particles. For channeled electrons, $A_{n,\kappa}$ is probably somewhat larger than A_{MS} because the overlap between the electrons and the vibrating nuclei is enhanced. Conversely, for channeled positrons, $A_{n,\kappa}$ is probably somewhat less than A_{MS}.

In order to simplify the analysis, we lump together the parameters $A_{n,\kappa}$ into a single phenomenological propor-

tionality constant $A_{\mathrm{MS;ch}}$; the corresponding multiple-scattering distribution for channeled particles is designated by

$$\Theta_{\mathrm{MS;ch}}(\theta_e;z)=A_{\mathrm{MS;ch}}z^{1/2}. \tag{3}$$

The multiple-scattering distribution must be convolved with the differential cross section for channeling radiation. If, as in Eq. (3), the multiple-scattering distribution is assumed to be independent of the initial state, the total ideal channeling-radiation spectrum can be convolved with $f_{\mathrm{MS;ch}}$ (rather than performing a convolution with $f_{n,\kappa}$ for each transition and then adding the individual transitions). One can show that, to a very good approximation, the differential channeling-radiation cross section can be expressed in terms of the differential cross section in the forward direction:[14]

$$\frac{d^3N_{\mathrm{CR}}(E_\gamma,\Omega_\gamma)}{dE_\gamma d\Omega_\gamma dz}=\left[\frac{\sin^2\phi_\gamma+(1-\theta_\gamma^2\gamma^2)^2/(1+\theta_\gamma^2\gamma^2)^2\cos^2\phi_\gamma}{(1+\theta_\gamma^2\gamma^2)^2}\right]\frac{d^3N_{\mathrm{CR}}((1+\theta_\gamma^2\gamma^2)E_\gamma,\mathbf{0})}{dE_\gamma d\Omega_\gamma dz}, \tag{4}$$

where the angle of the emitted photon with respect to the particle direction is denoted $\Omega_\gamma=(\theta_\gamma,\phi_\gamma)$ and ϕ_γ is measured with respect to the $\hat{\mathbf{x}}$ direction. Since the angles involved are quite small, spherical geometry can be replaced by Euclidean geometry, and the angles can be described as two-dimensional Euclidean vectors projected onto the plane perpendicular to the $\hat{z}$ direction.

The CR spectrum observed in the forward direction ($\Omega=\mathbf{0}$) is calculated by first convolving the multiple-scattering distribution $f_{\mathrm{MS;ch}}$ of Eq. (3) with the total ideal CR cross section given by substituting into Eq. (4) the CR differential cross section in the forward direction:

$$\frac{d^3N_{\mathrm{CR}}(i\to f)}{d\Omega_\gamma dE_\gamma dz}=\frac{\alpha\lambda_c^2}{\pi\hbar c}\frac{E_\gamma}{2\gamma^2(1-\beta\cos\theta)}\left[\sin^2\phi+\left[\frac{\cos\theta-\beta}{1-\beta\cos\theta}\right]^2\cos^2\phi\right]|M_{fi}|^2\delta\left[E_\gamma-\frac{\varepsilon_i-\varepsilon_f}{1-\beta\cos\theta}\right], \tag{5}$$

where $d\Omega_\gamma$ is the differential solid angle of the observed photon, dz is the differential crystal thickness, and M_{fi} is the matrix element:

$$M_{fi}=\left\langle u_f\left|e^{-iq_xx}\frac{d}{dx}\right|u_i\right\rangle\approx\left\langle u_f\left|\frac{d}{dx}\right|u_i\right\rangle. \tag{6}$$

(The approximate equality represents the usual dipole approximation, in which the $\hat{x}$ component of the photon's wave vector, q_x, is set equal to zero.) Then, after allowing for photon absorption in the crystal and the finite occupation length of channeled particles, the result is integrated over the thickness of the crystal. Since ϕ_e is constrained to be 90° and $\Omega=\Omega_\gamma+\Omega_e=\mathbf{0}$, the numerator of Eq. (4) simplifies to 1, and the full expression for the channeling-radiation spectrum observed in the forward direction from multiply scattered particles is

$$\frac{d^2N_{\mathrm{CR;MS}}(E_\gamma,\mathbf{0})}{dE_\gamma d\Omega_\gamma}=\int_0^Z dz\int_{-\infty}^{\infty}d\theta\, f_{\mathrm{MS;ch}}(\theta;z)\frac{e^{-\mu(E_\gamma)(Z-z)}e^{-z/L_{\mathrm{occ}}}}{(1+\theta^2\gamma^2)^2}\frac{d^3N_{\mathrm{CR}}((1+\theta^2\gamma^2)E_\gamma,\mathbf{0})}{dE_\gamma d\Omega_\gamma dz}, \tag{7}$$

where Z is the crystal thickness, $\mu(E_\gamma)$ is the photon absorption coefficient,[15] and L_{occ} is the occupation length of the channeled particles.

There are two undetermined parameters in Eq. (7)—the multiple-scattering proportionality constant $A_{\mathrm{MS;ch}}$ which appears in $f_{\mathrm{MS;ch}}(\theta_e;z)$ in Eq. (3) and the occupation length L_{occ}. $A_{\mathrm{MS;ch}}$ is taken to be equal to the value for unchanneled electrons passing through silicon, A_{MS}. This is almost certainly an underestimate, but in Ref. 8 it has been shown that the actual value is probably less than $2A_{\mathrm{MS}}$. The occupation length, the length scale over which channeled particles become dechanneled, has been measured for 16.9- and 54.5-MeV electrons for both the (100) and (110) planes of silicon.[8] Linear interpolation between the 16.9- and 54.5-MeV results yields estimates of the occupation lengths for 20.0- and 30.5-MeV electrons. The values which were assumed for $A_{\mathrm{MS;ch}}$ and L_{occ} are given in Table II. The crystal used for the 16.9- and 20.0-MeV experiments was approximately 10 μm thick; the one used for the 30.5- and 54.5-MeV experiments was approximately 20 μm thick.

Figure 2 illustrates the effect of the multiple-scattering correction on the calculated CR spectrum of 30.5-MeV electrons channeled along the (110) planes of a 20-μm-thick silicon crystal. For purposes of comparison, the ideal spectrum has been multiplied by an effective thick-

TABLE II. Parameters $A_{\mathrm{MS;ch}}$ and L_{occ} used in multiple-scattering calculations.

Beam energy (MeV)	$A_{\mathrm{MS;ch}}$ (mrad/μm$^{1/2}$)	L_{occ}(μm) (100)	(110)
16.9	2.5	16	20
20.0	2.15	17	21
30.5	1.4	20	28
54.5	0.8	24	36

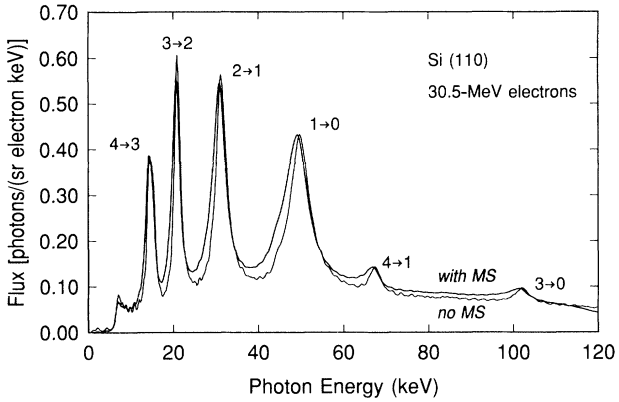

FIG. 2. The effect of the multiple-scattering correction on the calculated spectrum of Fig. 1. The uncorrected (gray) and corrected (solid) calculated spectra are displayed together for comparison. The multiple-scattering correction assumes a crystal thickness of 20 μm, an occupation length of 28 μm, and $A_{\mathrm{MS;ch}}=1.4$.

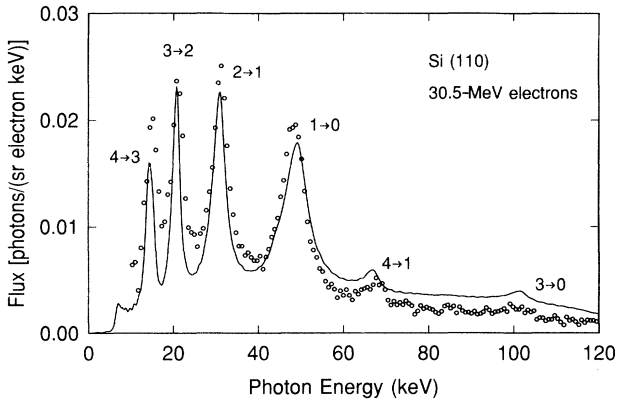

FIG. 3. Calculated spectrum with multiple-scattering correction from Fig. 2 (solid curve) and observed channeling-radiation spectrum of 30.5-meV electrons channeled along Si(110). The $1\rightarrow0$ and $3\rightarrow0$ transitions still fail to match the observed spectrum to within experimental error.

ness of 14 μm. As expected, the peaks acquire low-energy tails and the maxima shift downward somewhat. The magnitudes of these downward shifts, given in Table III, are approximately 1%. These multiple-scattering-corrected results are compared with the data in Fig. 3. One sees that the agreement for the $1\rightarrow0$ and $3\rightarrow0$ transitions, although improved somewhat, is still unsatisfactory.

C. Thermal-vibrational amplitudes

To reconcile the calculated $1\rightarrow0$ and $3\rightarrow0$ energies with the observed energies, one must raise the level of the $n=0$ state without affecting the other states. Thus, it is necessary to increase the calculated crystal potential in the region where the $n=0$ state is concentrated—in the vicinity of the atomic nuclei. This can be done by increasing the one-dimensional projection of the root-mean-square vibration amplitude u, often called the "thermal vibrational amplitude," in the direction perpendicular to the planes. The effect of u on the continuum potential is illustrated in Fig. 4. If the atoms were completely frozen in the lattice, the continuum potential would have the cusplike shape shown in the figure. (Note that even in the absence of vibrations, the planar continuum potential is far from being singular; it is only about 26 eV deep.) However, a frozen lattice is impossible, since zero-point vibrations of the crystal lattice broaden the continuum potential substantially.

According to the *International Tables for X-Ray Crystallography*, $u=0.075$ Å for crystalline silicon at room temperature,[16] a result obtained from x-ray diffraction measurements.[17] The thermally averaged planar potential $V(x)$ for the Si(110) plane based upon this value of u is superimposed on the frozen-lattice potential in Fig. 4. The depth of the thermally averaged potential is reduced in the region $|x|<u$ (where the interplanar distance x is measured from the nucleus) and essentially unchanged in the region $|x|>u$.

As shown in Fig. 5, when the thermal-vibrational amplitude is increased from $u=0.075$ to 0.081 Å, the $n=0$ energy eigenvalue increases from -17.07 to -16.87 eV, while the other energies are virtually unaffected. The calculated spectrum based upon this revised thermal-vibrational amplitude of $u=0.081$ Å is displayed in Fig. 6, with the measured spectrum superimposed upon it as before. Now the positions of all six of the calculated bound-bound peaks agree with observation to within the experimental uncertainty.

The physical significance of this revised thermal-vibrational amplitude was investigated by observing the CR spectra of electrons with four different energies—16.9, 20.0, 30.5, and 54.5 MeV—for both the (110) and

TABLE III. Calculated photon-energy downshifts due to multiple scattering for 30.5-MeV ($\gamma=60.78$) electrons channeled along the (110) planes of Si. The crystal is assumed to be 20 μm thick.

Transition	$E_{\gamma(\mathrm{calc})}$ (keV) (no MS)	$E_{\gamma(\mathrm{calc})}$ (keV) (with MS)	Downshift (keV)	Downshift (%)
$(4\rightarrow3)_{(110)}$	14.76	14.55	0.21	1.4
$(3\rightarrow2)_{(110)}$	20.98	20.74	0.24	1.1
$(2\rightarrow1)_{(110)}$	31.22	30.88	0.34	1.1
$(1\rightarrow0)_{(110)}$	49.76	49.08	0.64	1.3
$(4\rightarrow1)_{(110)}$	67.33	66.76	0.57	0.8
$(3\rightarrow0)_{(110)}$	102.05	101.09	0.96	0.9

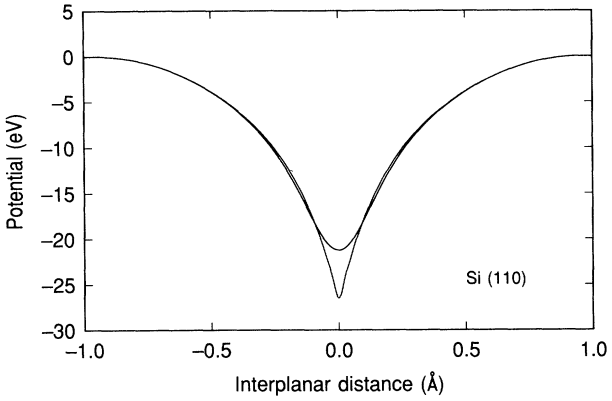

FIG. 4. Continuum potentials for the (110) plane of silicon assuming frozen lattice (cusplike gray curve) and thermal-vibrational amplitude $u = 0.075$ Å (solid curve).

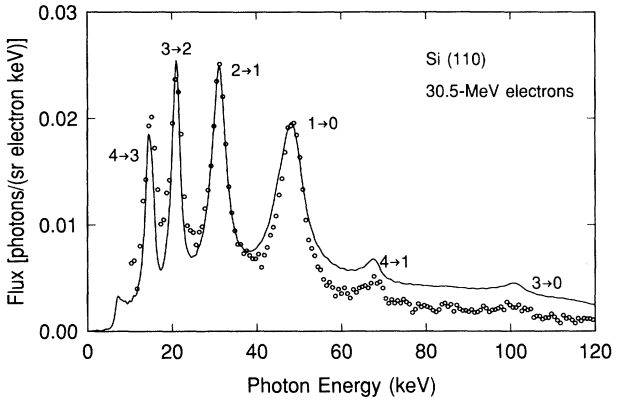

FIG. 6. Same as Fig. 3, except that u has been increased from 0.075 to 0.081 Å. Now the $1\rightarrow0$ and $3\rightarrow0$ transitions match the observed spectrum to within experimental error.

the (100) planes of silicon. By varying the energy of the incident electron beam, one can alter the energies of the eigenstates and thus sample different parts of the continuum potential (see Figs. 7 and 8). However, since the thermal-vibrational amplitude is an intrinsic property of the crystal, the same thermal-vibrational amplitude ought to fit the data for all beam energies.

When the calculated (using $u = 0.075$ Å) and observed CR spectra are compared, we find that, in every case, the agreement is excellent *except* for those transitions which involve $n = 0$, in which case the calculated peak is significantly too high. This encourages us to seek a single revised thermal-vibrational amplitude which is capable of fitting the data for all four beam energies.

First, however, it is necessary to obtain as accurate as possible an estimate of the electron-beam energy. The nominal beam energy, which is estimated to be accurate to within $\pm 0.75\%$, is obtained by measuring the current in the bending magnet used for energy selection and interpolating a calibrated curve relating energy to current.

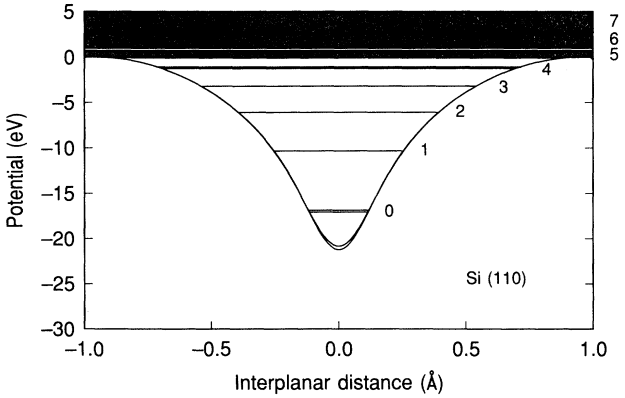

FIG. 5. Continuum potentials for the (110) plane of silicon assuming $u = 0.075$ Å (gray curve) and $u = 0.081$ Å (solid curve), along with transverse energy eigenvalues for both potentials. The only noticeable difference is in the $n = 0$ state, which is slightly higher in energy for $u = 0.081$ Å.

Our theoretical understanding of the energies of channeling-radiation peaks and our ability to measure them accurately are sufficiently advanced to allow us to use the channeling-radiation measurements themselves to refine our estimate of the beam energy.

For example, the calculated energies of the $4\rightarrow3$, $3\rightarrow2$, $2\rightarrow1$, and $4\rightarrow1$ transitions for $\gamma = 60.78$ electrons channeled by the (110) planes of silicon are displayed in

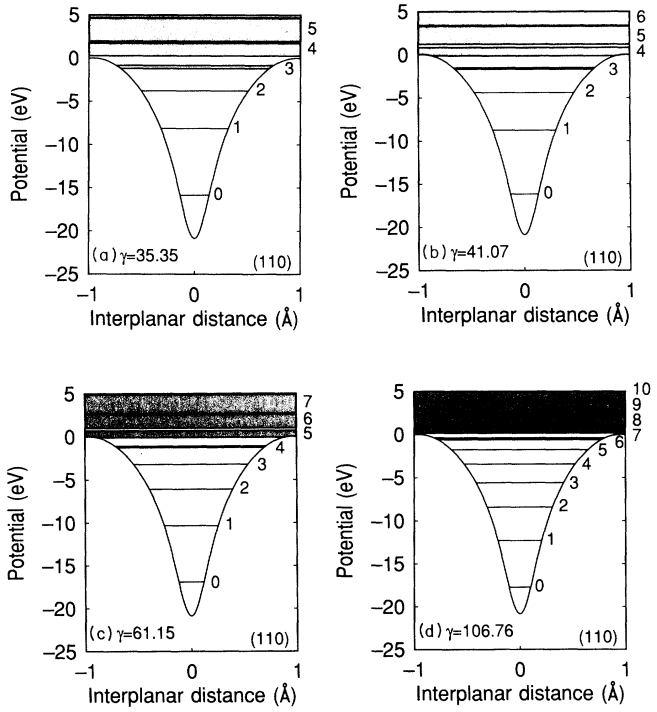

FIG. 7. Continuum potential for the Si(110) plane, assuming $u = 0.0813$ Å, with transverse-energy eigenvalues for beam energies of (a) $\gamma = 35.35$, (b) $\gamma = 41.07$, (c) $\gamma = 61.15$, and (d) $\gamma = 106.76$. Shaded areas near the tops of the potential wells denote energy bands, which arise from the dependence of energy upon transverse momentum.

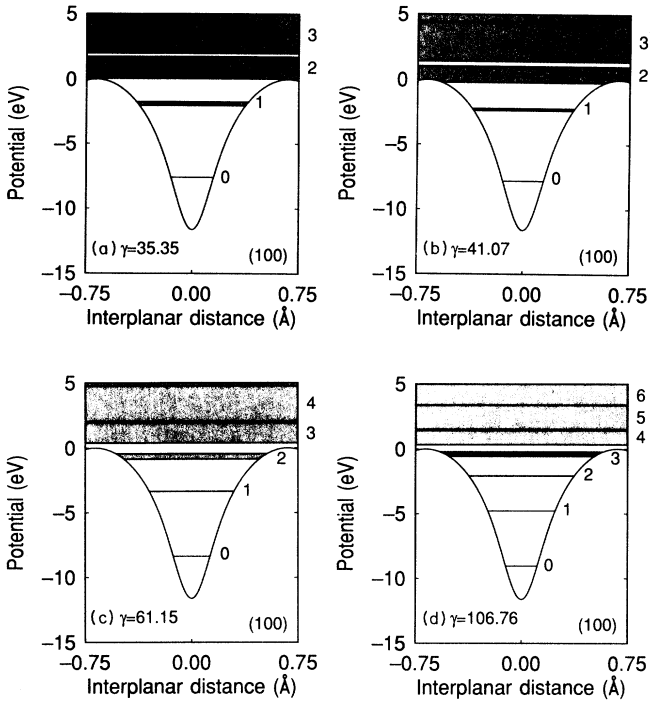

FIG. 8. Continuum potential for the Si(100) plane, assuming $u=0.0789$ Å, with transverse-energy eigenvalues for beam energies of (a) $\gamma=35.35$, (b) $\gamma=41.07$, (c) $\gamma=61.15$, and (d) $\gamma=106.76$.

the second column of Table IV, along with the $2\rightarrow1$ transition for the (100) plane. A thermal-vibrational amplitude of $u=0.075$ Å has been assumed. (Transitions involving the $n=0$ state have been excluded because they are too sensitive to the exact choice of the thermal-vibrational amplitude.) The calculated derivatives of the CR photon energies with respect to γ and u are given in the third and fourth columns. Since the derivatives with respect to u are very small for these five transitions, the derived value of γ is fairly insensitive to the thermal-vibrational amplitude. The measured photon energies, along with their estimated uncertainties, are displayed in the fifth column. For each transition, one can determine the value of γ which best fits the observed photon energy for that transition. After combining these estimates, it is found that the overall best estimate is $\gamma=61.12\pm0.12$, which is in good agreement with the nominal beam energy of $\gamma=60.78$.

Having established the beam energy, the values of u which best fit the measured $1\rightarrow0$ and $3\rightarrow0$ transition energies for the (110) plane and the $1\rightarrow0$ transition energy for the (100) plane now can be determined. The calculated energies for these three transitions (assuming $\gamma=60.78$ and $u=0.075$ Å), along with their derivatives with respect to γ and u, also are included in Table IV. Note that the derivatives dE_γ/du are nearly 2 orders of magnitude greater for the transitions which involve the $n=0$ state than for those which do not. After using the derivatives $dE_\gamma/d\gamma$ to make a slight adjustment to the calculated energies E_γ, the derivatives dE_γ/du can be used to determine the value of u which best fits the observed photon energy. Using this procedure, the best fit for the (110) plane is $u=0.0815\pm0.0014$ Å, while for the (100) plane, $u=0.0787\pm0.0015$ Å.

Following the same procedure for the three other beam energies—16.9, 20.0, and 30.5 MeV—and performing a statistically weighted average of the results based upon the individual uncertainties at each beam energy, we obtain $u=0.0824\pm0.0014$ Å for the (110) plane and $u=0.0789\pm0.0007$ Å for the (100) plane. However, these results cannot be regarded as final because the revised vibrational amplitudes deviate so substantially from $u=0.075$ Å that the derivative d^2E_γ/du^2 may be important, particularly for the (110) plane. In particular, in the case of the 54.5-MeV (110) data, transitions involving the $n=1$ state have a significant dependence upon u—about 20% as strong as those involving the $n=0$ state. At this energy, the $n=1$ state has become sufficiently localized near the nuclei to be influenced by thermal vibra-

TABLE IV. Calculated and observed channeling-radiation peak energies for 30.5-MeV electrons channeled along the (100) and (110) planes of Si, along with derived best-fit values of γ and the thermal-vibrational amplitude u. The nominal value of $\gamma=60.78$; the overall best-fit value obtained from sixth column is $\gamma=61.12\pm0.12$. The calculated energies in the second column are based upon the nominal γ and $u=0.075$ Å. Multiple scattering has been included in the calculation.

Transition	$E_{\gamma(\text{calc})}$ (keV)	$dE_\gamma/d\gamma$ (keV)	dE_γ/du (keV/Å)	$E_{\gamma(\text{obs})}$ (keV)	$\gamma_{(\text{fit})}$	$u_{(\text{fit})}$ (Å)
$(4\rightarrow3)_{(110)}$	14.60	0.55	−1.0	14.9±0.2	61.33±0.36	
$(3\rightarrow2)_{(110)}$	20.78	0.70	−1.3	21.1±0.2	61.24±0.29	
$(2\rightarrow1)_{(110)}$	30.93	0.98	−10.9	31.1±0.2	60.95±0.20	
$(4\rightarrow1)_{(110)}$	66.91	2.22	−10.6	66.8±0.5	60.81±0.23	
$(2\rightarrow1)_{(100)}$	18.90	0.69	−4.5	19.55±0.2	61.72±0.29	
$(1\rightarrow0)_{(110)}$	49.30	1.35	−229.3	48.4±0.3		0.0809±0.0015
$(3\rightarrow0)_{(110)}$	101.61	3.02	−234.5	100.2±0.8		0.0854±0.0037
$(1\rightarrow0)_{(100)}$	37.31	1.07	−162.5	37.06±0.2		0.0787±0.0015

tions. In order to obtain a reasonable estimate of γ from the 54.5-MeV Si(110) $2\rightarrow1$ and $4\rightarrow1$ transitions, it is necessary to start from a good estimate of u for the (110) plane. Therefore, we have iterated the above procedure once more, starting from the revised vibrational amplitudes mentioned above. The results for all four beam energies are given in Table V.

The best-fit thermal-vibrational amplitudes for each energy and plane are summarized in Table VI. Note that the error bars are smaller for the higher beam energies. At higher beam energies, the increased localization of the $n=0$ wave function makes it more sensitive to the details of the potential in the vicinity of the vibrating nuclei. In addition, the approximate $\gamma^{1.7}$ dependence of the $1\rightarrow0$ peak energy outpaces the $\gamma^{0.5}$ dependence of the germanium detector resolution, so that the relative measurement uncertainty decreases approximately linearly with energy.

According to Table VI, the overall best fits are $u=0.0813\pm0.0009$ Å for the (110) plane and $u=0.0789\pm0.0007$ Å for the (100) plane. Since the mean values are separated by about *three standard deviations,* the anisotropy is statistically significant. In order to check how well a single value of u is able to fit the data for four different beam energies, the observed peak energies were compared with the calculated peak energies for the (100) and (110) planes. For the published value of $u=0.075$ Å, the errors for the $1\rightarrow0$ transition energy are enormous—ranging as high as seven standard deviations or more for the (110) plane. In this case, the reduced χ^2 value is approximately 10 for both the (110) and (100) planes. For the revised thermal-vibrational amplitudes, the individual errors rarely exceed one standard deviation, and the overall reduced χ^2 is somewhat less than one in both cases, indicating that the fit is very good.

III. RESULTS AND DISCUSSION

After performing this analysis for all four electron-beam energies and both planes, using the average

TABLE V. Derivation of beam energies and thermal-vibrational amplitudes from observed channeling-radiation peak energies for 16.9-, 20.0-, 30.5-, and 54.5-MeV electrons channeled along the (110) and (100) planes of Si, along with derived best-fit values of γ and the thermal-vibrational amplitude u. The nominal values of γ are given in the first column; the best-fit values obtained from the fourth column are given in parentheses. Multiple scattering has been included in the calculation.

γ	Transition	$E_{\gamma(\text{obs})}$ (keV)	$\gamma_{(\text{fit})}$	$u_{(\text{fit})}$ (Å)
34.11 (35.35±0.17)	$(3\rightarrow2)_{(110)}$	7.0±0.4	36.35±0.97	
	$(2\rightarrow1)_{(110)}$	10.7±0.1	35.32±0.17	
	$(1\rightarrow0)_{(110)}$	18.9±0.1		0.0838±0.0029
	$(3\rightarrow0)_{(110)}$	36.5±0.2		0.0853±0.0041
	$(1\rightarrow0)_{(100)}$	13.95±0.1		0.0804±0.0036
40.23 (41.07±0.24)	$(3\rightarrow2)_{(110)}$	9.2±0.2	41.23±0.42	
	$(2\rightarrow1)_{(110)}$	14.4±0.2	40.99±0.29	
	$(1\rightarrow0)_{(110)}$	24.6±0.2		0.0831±0.0033
	$(3\rightarrow0)_{(110)}$	48.2±0.3		0.0852±0.0066
	$(1\rightarrow0)_{(100)}$	18.2±0.1		0.0818±0.0029
60.78 (61.15±0.12)	$(4\rightarrow3)_{(110)}$	14.9±0.2	61.70±0.36	
	$(3\rightarrow2)_{(110)}$	21.1±0.2	61.22±0.29	
	$(2\rightarrow1)_{(110)}$	31.1±0.2	61.09±0.20	
	$(4\rightarrow1)_{(110)}$	66.8±0.5	60.85±0.23	
	$(2\rightarrow1)_{(100)}$	19.55±0.2	61.32±0.29	
	$(1\rightarrow0)_{(110)}$	48.4±0.3		0.0804±0.0015
	$(3\rightarrow0)_{(110)}$	100.2±0.8		0.0833±0.0037
	$(1\rightarrow0)_{(100)}$	37.06±0.2		0.0781±0.0015
107.56 (106.76±0.15)	$(5\rightarrow4)_{(110)}$	36.8±0.6	106.12±0.76	
	$(4\rightarrow3)_{(110)}$	48.6±0.6	107.32±0.65	
	$(3\rightarrow2)_{(110)}$	63.5±0.5	106.77±0.43	
	$(2\rightarrow1)_{(110)}$	87.3±0.5	106.87±0.31	
	$(5\rightarrow2)_{(110)}$	149.8±2.5	106.95±0.85	
	$(4\rightarrow1)_{(110)}$	198.4±2.0	106.67±0.54	
	$(3\rightarrow2)_{(100)}$	36.8±0.4	106.43±0.48	
	$(2\rightarrow1)_{(100)}$	60.9±0.3	106.76±0.25	
	$(1\rightarrow0)_{(110)}$	120.2±1.0		0.0804±0.0015
	$(1\rightarrow0)_{(100)}$	95.7±0.4		0.0789±0.0009
	$(3\rightarrow0)_{(100)}$	193.3±2.0		0.0773±0.0036

TABLE VI. Derived thermal-vibrational amplitudes for the (100) and (110) planes of Si, including multiple-scattering correction.

Beam energy (γ)	(100) (Å)	(110) (Å)
35.32	0.0804±0.0036	0.0841±0.0025
41.07	0.0818±0.0029	0.0835±0.0030
61.15	0.0781±0.0015	0.0808±0.0014
106.76	0.0788±0.0009	0.0804±0.0015
Overall best fits:	0.0789±0.0007	0.0813±0.0009

thermal-vibrational amplitudes from Table VI, a final set of calculated transition energies has been obtained and compared with the measured energies for the (110) and (100) planes in Tables VII and VIII, respectively. The values of χ^2, given in the last column of these tables, are close to one for both planes, indicating that the fits are very good.

The final results are shown graphically in Figs. 7–10. Figures 7 and 8 show the transverse energy eigenvalues calculated for the (110) and (100) planes, respectively, using the final values for γ and u given in Table VI. Figures 9 and 10 show the measured channeling-radiation spectra for the (110) and (100) planes, respectively, compared with the spectra calculated using the potentials and eigenvalues of Figs. 7 and 8.

Although there is some uncertainty about the exact values of $A_{\mathrm{MS;ch}}$ and L_{occ}, which ought to be inserted into Eqs. (3) and (6), we have verified that the derived thermal-vibrational amplitudes are essentially unchanged even when the effects of multiple scattering, occupation length, and photon absorption are completely neglected in the calculation. The following intuitive argument explains this insensitivity. Although the multiple-scattering angle $\Theta_{\mathrm{MS}}(z)$ is a function of the penetration depth z, the total multiple scattering which occurs throughout the thickness of a crystal can be characterized by some average multiple-scattering angle $\Theta_{\mathrm{MS;av}}$. Due mainly to the diminution of the intensity of radiation emitted off axis (given by the factor of $[1+(\gamma\Theta_{\mathrm{MS;av}})^2]^{-2}$ in Eq. (4)) and also partly to the finite occupation length, $\Theta_{\mathrm{MS;av}}$ is significantly smaller than the value that one would obtain from the more obvious assumption $\Theta_{\mathrm{MS;av}}\approx\Theta_{MS}(Z)/2$. The channeling-radiation spectrum will shift downward by a factor of approximately $[1+(\gamma\Theta_{\mathrm{MS;av}})^2]^{-1}$. Consequently, multiple scattering will cause all of the peaks of a given spectrum to shift downward by approximately the same percentage—a fact which is apparent from Table III.

This same downward shift can be mimicked closely in calculations which do not include multiple scattering

TABLE VII. Calculated and observed channeling-radiation peak energies for electrons channeled along the (110) planes of Si. Calculated energies are based upon the best-fit values of γ for each beam energy and the derived value of u given in Table VI, with multiple scattering taken into account. The deviations of the calculated from the observed energies are given in standard deviations.

γ	Transition	$E_{\gamma(\mathrm{calc})}$ (keV) ($u=0.0813$ Å)	$E_{\gamma(\mathrm{obs})}$ (keV)	Deviation (st. dev.)
35.35	$(3\rightarrow2)_{(110)}$	6.59	7.0±0.4	−1.0
	$(2\rightarrow1)_{(110)}$	10.72	10.7±0.1	0.2
	$(1\rightarrow0)_{(110)}$	19.07	18.9±0.1	1.7
	$(3\rightarrow0)_{(110)}$	36.71	36.5±0.2	1.1
41.07	$(3\rightarrow2)_{(110)}$	9.12	9.2±0.2	−0.4
	$(2\rightarrow1)_{(110)}$	14.46	14.4±0.2	0.3
	$(1\rightarrow0)_{(110)}$	24.78	24.6±0.2	0.9
	$(3\rightarrow0)_{(110)}$	48.56	48.2±0.3	1.2
61.15	$(4\rightarrow3)_{(110)}$	14.60	14.9±0.2	−1.5
	$(3\rightarrow2)_{(110)}$	21.05	21.1±0.2	−0.3
	$(2\rightarrow1)_{(110)}$	31.17	31.1±0.2	0.4
	$(1\rightarrow0)_{(110)}$	48.21	48.4±0.3	−0.6
	$(4\rightarrow1)_{(110)}$	67.47	66.8±0.5	1.3
	$(3\rightarrow0)_{(110)}$	100.70	100.2±0.8	0.6
106.76	$(5\rightarrow4)_{(110)}$	37.31	36.8±0.6	0.8
	$(4\rightarrow3)_{(110)}$	48.08	48.6±0.6	−0.9
	$(3\rightarrow2)_{(110)}$	63.49	63.5±0.5	0.0
	$(2\rightarrow1)_{(110)}$	87.30	87.3±0.5	0.0
	$(1\rightarrow0)_{(110)}$	119.65	120.2±1.0	−0.5
	$(5\rightarrow2)_{(110)}$	149.26	149.8±2.5	−0.2
	$(4\rightarrow1)_{(110)}$	198.93	198.4±2.0	0.3
Reduced χ^2:				0.95

TABLE VIII. Calculated and observed channeling-radiation peak energies for electrons channeled along the (100) planes of Si. The calculated energies are based upon the best-fit values of γ for each beam energy and the derived value of u given in Table VI, with multiple scattering taken into account. The deviations of the calculated from the observed energies are given in standard deviations.

γ	Transition	$E_{\gamma(\text{calc})}$ (keV) ($u=0.0789$ Å)	$E_{\gamma(\text{obs})}$ (keV)	Deviation (st. dev.)
35.35	$(1\rightarrow0)_{(100)}$	14.04	13.95±0.1	0.9
41.07	$(1\rightarrow0)_{(100)}$	18.38	18.2±0.1	1.8
61.15	$(2\rightarrow1)_{(100)}$	19.43	19.55±0.2	−0.6
	$(1\rightarrow0)_{(100)}$	36.93	37.06±0.2	−0.7
106.76	$(3\rightarrow2)_{(100)}$	37.08	36.8±0.4	0.7
	$(2\rightarrow1)_{(100)}$	60.89	60.9±0.3	0.0
	$(1\rightarrow0)_{(100)}$	95.69	95.7±0.4	0.0
	$(3\rightarrow0)_{(100)}$	192.37	193.3±2.0	−0.5
Reduced χ^2:				0.93

simply by assuming that γ is slightly smaller than its actual value. The reason is that the γ dependence of the CR peak energies is nearly independent of which transition is being considered. CR peak energies are proportional to γ^{α}, where α is an exponent which ranges from about 1.7 for the $1\rightarrow0$ transitions to about 2.0 for the transitions which involve states lying near the top of the potential well.[5,18] The derivative of the photon energy with respect to γ for a peak at an energy E_γ is $\alpha\gamma^{-1}E_\gamma$. Aside from the slight variation of α between 1.7 and 2.0, this is very nearly proportional to the photon energy—that is, a small variation in γ will cause all peaks to shift by approximately the same percentage.

Since both multiple scattering and a variation in γ shift the CR peaks by an amount which is approximately proportional to their energy, and since γ is allowed to vary in the data fitting, the multiple-scattering effects can be absorbed into an effective value of γ which is slightly lower than the actual value. Also, by the same argument, a slight misalignment of the detector could be absorbed into a lower effective γ. Therefore, the proper adjust-

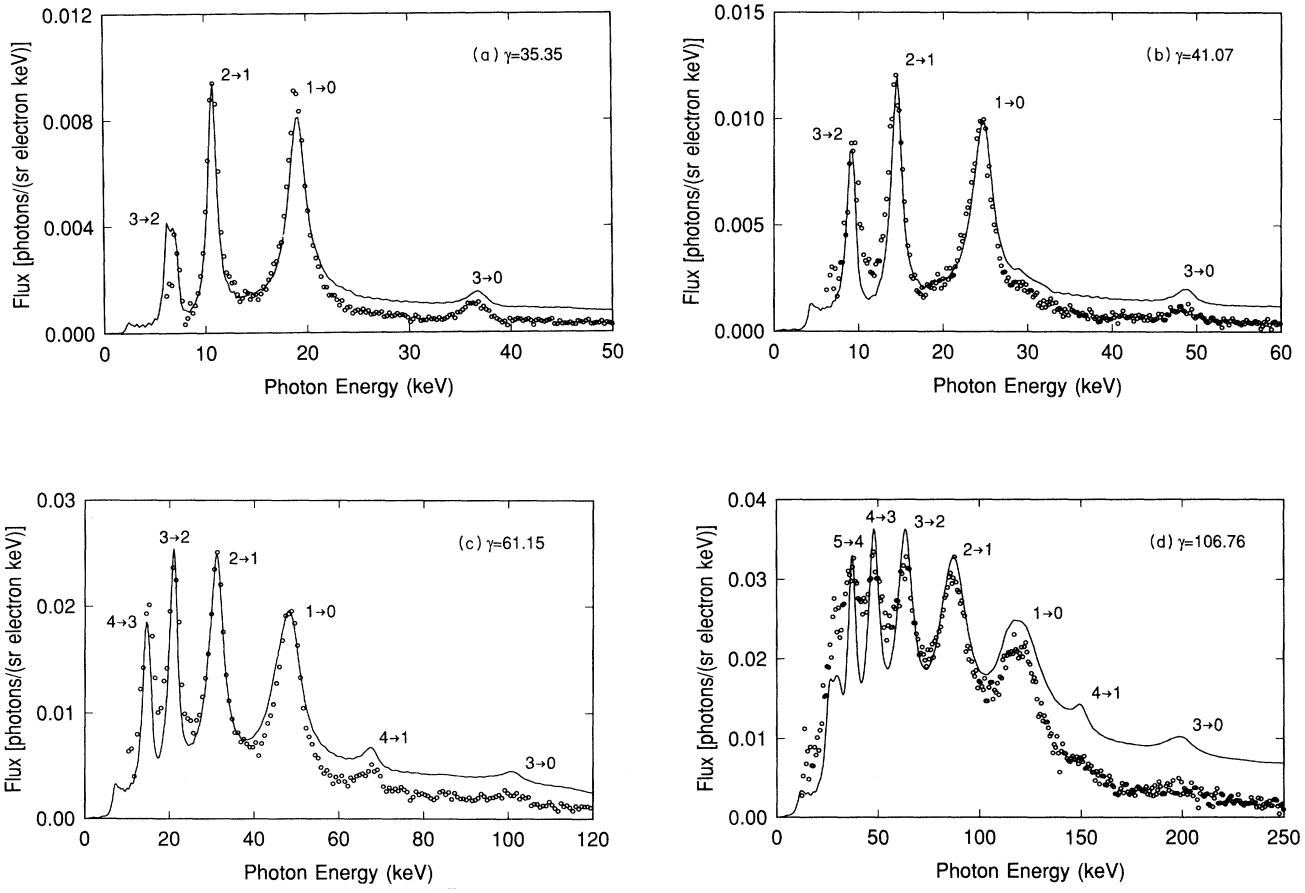

FIG. 9. Calculated (solid curve) and observed channeling-radiation spectra of (a) $\gamma=35.35$, (b) $\gamma=41.07$, (c) $\gamma=61.15$, and (d) $\gamma=106.76$ electrons channeled along the (110) planes of silicon. Calculation assumes vibrational amplitude $u=0.0813$ Å and includes multiple-scattering correction using the parameters of Table II. Assumed crystal thicknesses are 10 μm for (a) and (b) and 20 μm for (c) and (d).

ment of the $1\rightarrow0$ and $3\rightarrow0$ peak energies relative to the other peaks depends almost entirely upon the thermal-vibrational amplitude.

The results $u=0.0813\pm0.0009$ Å for the (110) plane and $u=0.0789\pm0.0007$ Å for the (100) plane are in reasonable agreement with a previous channeling-radiation measurement[7] of the Debye temperature of silicon taken at an electron-beam energy of 54.5 MeV at crystal temperatures ranging from 80 to 293 K. From the measured Debye temperature of 495 ± 10 K (the planes were not distinguished), the corresponding vibration amplitude at room temperature is 0.0819 ± 0.0015 Å).

The discrepancy between both of these values and the published value of $u=0.075\pm0.001$ Å, which is based upon x-ray-diffraction measurements,[16] is not yet understood. Such discrepancies have not been observed for other crystals with the same crystal structure, such as diamond, germanium, and gallium arsenide.[4] The best available calculations of the thermal-vibrational amplitude of silicon, which fail to differentiate among various planes, lie between the x-ray and CR results: $u=0.0768$ Å for the bond-charge model and 0.0776 Å for the shell model at a temperature of 290 K.[19] Our measurement of a statistically significant anisotropy of 3% demands greater sophistication from any future theoretical calculations.

Our results strongly suggest that thermal-vibrational amplitudes in crystals can be determined very accurately by measuring the positions of channeling-radiation peaks. There are a number of reasons to expect that this technique should provide results more accurate than those which can be obtained by x-ray diffraction. Whereas channeling radiation is sensitive to the *potential* of the crystal, x-ray-diffraction measurements are sensitive to the *electron distribution* in the crystal. Since the electron distribution and the potential are related through the Poisson equation, one might expect the x-ray-diffraction and channeling-radiation techniques to yield exactly the same result for the thermal-vibrational amplitude. However, the potential experienced by a channeled particle is due to both the atomic electrons and the atomic nuclei, whereas the contribution of the atomic nuclei to x-ray diffraction is negligible (about 6 orders of magnitude less) because the Thompson cross section is inversely proportional to the square of the mass of the scatterer.[20] There-

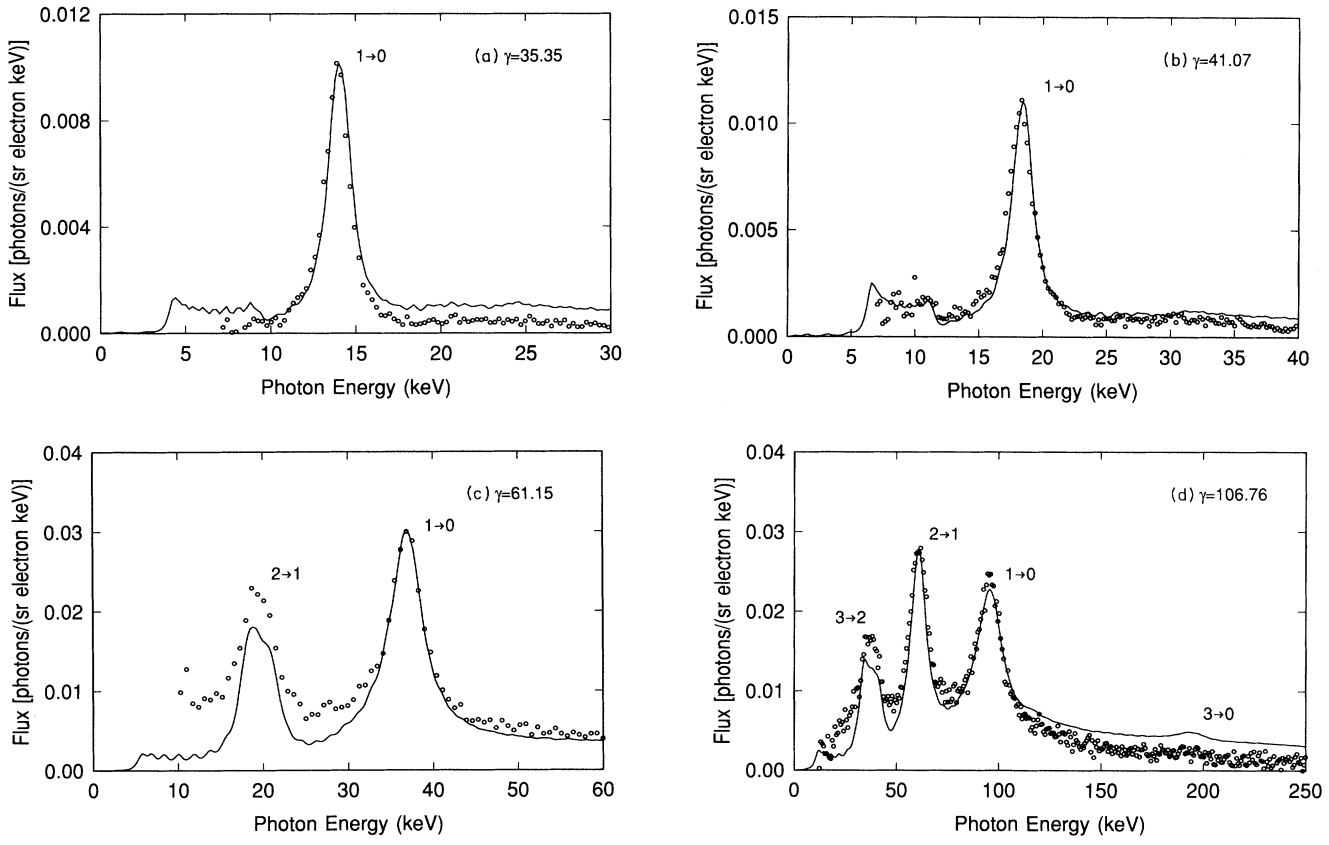

FIG. 10. Calculated (solid curve) and observed channeling-radiation spectra of (a) $\gamma=35.35$, (b) $\gamma=41.07$, (c) $\gamma=61.15$, and (d) $\gamma=106.76$ electrons channeled along the (100) planes of silicon. Calculation assumes vibrational amplitude $u=0.0789$ Å and includes multiple-scattering correction using the parameters of Table II. Assumed crystal thicknesses are 10 μm are (a) and (b) and 20 μm for (c) and (d).

fore, x rays can reveal information only about the electron clouds which surround the nuclei, whereas channeling radiation provides information about the atomic nuclei as well. If the rigid-atom model of crystal structure were not quite valid, the electrons would not respond perfectly to the vibrational motion of the nuclei, and their thermal-vibrational amplitude would be slightly less than that of the nuclei. This might explain why the x-ray measurements yield a smaller value of u than the channeling-radiation measurements.

The channeling-radiation technique possesses at least two inherent practical advantages over the x-ray technique. First, since the $n=0$ electron wave function is well-localized near the vibrating nuclei, it is much more sensitive to the vibrations than are x rays, which are nearly plane waves. Second, it is much easier and more reliable to measure the positions of CR peaks (which can be determined to within about 0.5%) than it is to measure the intensities of thousands of x-ray-diffraction peaks.[16,21] Diffracted intensities must be corrected for a variety of effects, such as absorption, extinction, and thermal diffuse scattering. These difficulties are acknowledged in the concluding paragraphs of *Thermal Vibrations in Crystallography:*[21] "the correction of x-ray intensities for the contribution of thermal diffuse scattering can be as large as 25 per cent, but the evaluation of the correction requires a knowledge of the elastic constants and the use of a theory which is built on numerous approximations." In fact, the inconsistencies between thermal parameters obtained by different x-ray-diffraction techniques has led Zachariasen to declare: "Looking at the many structures which have been published in *Acta Crystallographica* during the last few years, it is evident that the positional parameters are reasonably good... [but that] the thermal parameters are all nonsense and must all be done again in a sensible way."[22] Perhaps the "sensible" method sought by Zachariasen is to use channeling radiation.

ACKNOWLEDGMENTS

This work was supported by the U.S. Air Force Office of Scientific Research under Grant No. F49620-86-K-0015.

[1]B. L. Berman and S. Datz, in *Coherent Radiation Soures,* edited by A. W. Sáenz and H. Überall (Springer-Verlag, Heidelberg, 1985), p. 165.

[2]J. U. Andersen, E. Bonderup, and R. H. Pantell, Annu. Rev. Nucl. Part. Sci. **33**, 453 (1983).

[3]B. L. Berman, J. O. Kephart, R. H. Pantell, S. Datz, H. Park, R. K. Klein, and B. A. Dahling, in *Relativistic Channeling,* edited by Richard A. Carrigan, Jr. and James A. Ellison (Plenum, New York, 1987), p. 239.

[4]R. H. Pantell, J. O. Kephart, R. K. Klein, H. Park, B. L. Berman, and S. Datz, in *Relativistic Channeling,* edited by Richard A. Carrigan, Jr. and James A. Ellison (Plenum, New York, 1987), p. 435.

[5]R. K. Klein, J. O. Kephart, R. H. Pantell, H. Park, B. L. Berman, R. L. Swent, S. Datz, and R. W. Fearick, Phys. Rev. B **31**, 68 (1985).

[6]S. Datz, B. L. Berman, B. A. Dahling, M. V. Hynes, H. Park, J. O. Kephart, R. K. Klein, and R. H. Pantell, Nucl. Instrum. Methods B **13**, 19 (1986).

[7]H. Park, J. O. Kephart, R. K. Klein, R. H. Pantell, M. V. Hynes, B. L. Berman, B. A. Dahling, S. Datz, R. L. Swent, and M. J. Alguard, Phys. Rev. B **35**, 13 (1987).

[8]J. O. Kephart, R. H. Pantell, B. L. Berman, S. Datz, H. Park, and R. K. Klein, Phys. Rev. B **40**, 4249 (1989).

[9]J. O. Kephart, Ph.D. thesis, Stanford University, 1987.

[10]S. Satpathy (private communication).

[11]W. T. Scott, Rev. Mod. Phys. **35**, 256 (1963).

[12]V. L. Highland, Nucl. Instrum. Methods **129**, 497 (1975).

[13]E. V. Hungerford and B. W. Mayes, At. Nucl. Data Tables **15**, 477 (1975).

[14]D. M. Bird and B. F. Buxton, Proc. R. Soc. London Ser. A **379**, 459 (1982), in which there is a typographical error in the fraction which multiplies the $\cos^2\phi$ factor; it ought to be squared.

[15]E. F. Plechaty, D. E. Cullen, and R. J. Howerton (unpublished).

[16]*International Tables for X-Ray Crystallography,* 2nd ed., edited by N. F. M. Henry and K. Lonsdale (Kynoch, Birmingham, England, 1965).

[17]B. W. Batterman and D. R. Chipman, Phys. Rev. **127**, 681 (1964).

[18]R. L. Swent, R. H. Pantell, H. Park, J. O. Kephart, R. K. Klein, S. Datz, R. W. Fearick, and B. L. Berman, Phys. Rev. B **29**, 52 (1984).

[19]O. H. Nielsen and W. Weber, J. Phys. C **13**, 2449 (1980).

[20]J. D. Jackson, *Classical Electrodynamics,* 2nd ed. (Wiley, New York, 1975), p. 681.

[21]B. T. M. Willis and A. W. Pryor, *Thermal Vibrations in Crystallography* (Cambridge University, London, 1975).

[22]W. H. Zachariasen, Acta Crystallogr. A **25**, 276 (1969), as quoted in Willis and Pryor, Ref. 21.

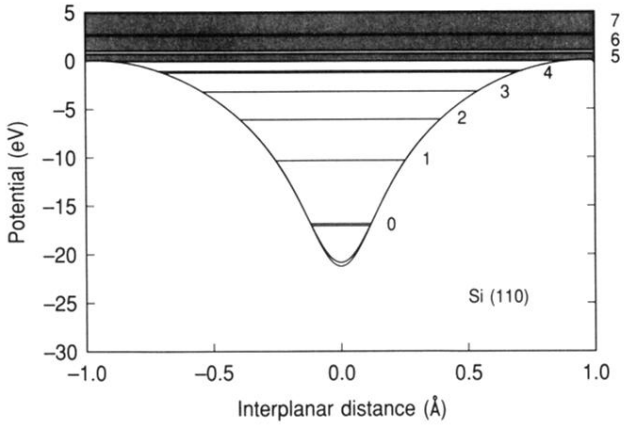

FIG. 5. Continuum potentials for the (110) plane of silicon assuming $u = 0.075$ Å (gray curve) and $u = 0.081$ Å (solid curve), along with transverse energy eigenvalues for both potentials. The only noticeable difference is in the $n = 0$ state, which is slightly higher in energy for $u = 0.081$ Å.

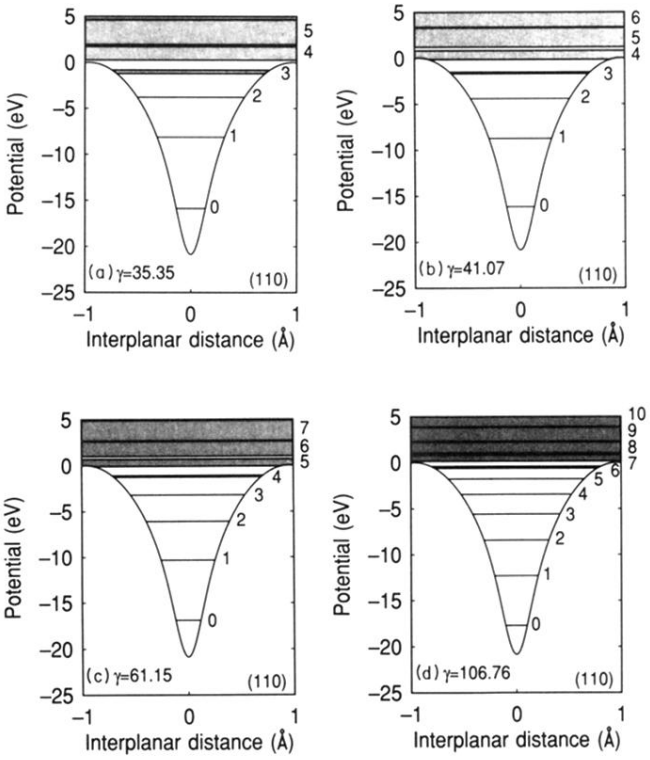

FIG. 7. Continuum potential for the Si(110) plane, assuming $u = 0.0813$ Å, with transverse-energy eigenvalues for beam energies of (a) $\gamma = 35.35$, (b) $\gamma = 41.07$, (c) $\gamma = 61.15$, and (d) $\gamma = 106.76$. Shaded areas near the tops of the potential wells denote energy bands, which arise from the dependence of energy upon transverse momentum.

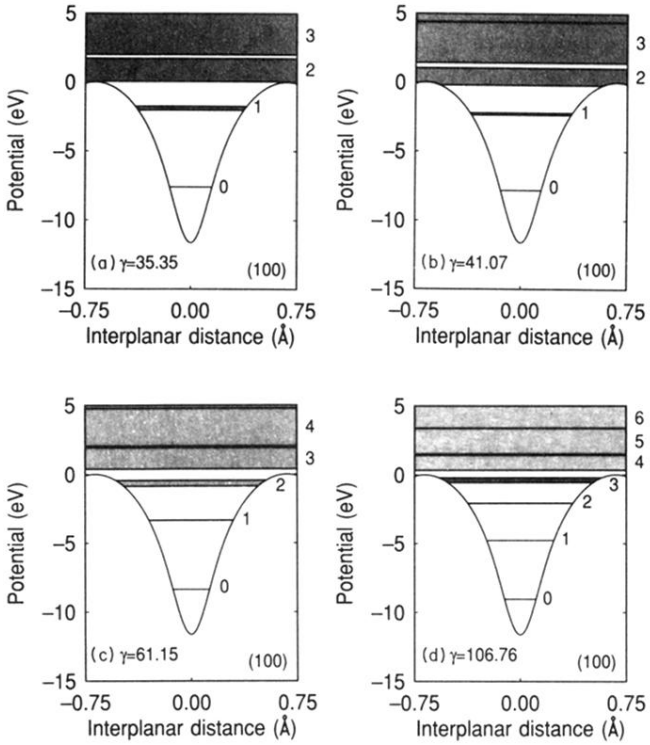

FIG. 8. Continuum potential for the Si(100) plane, assuming $u = 0.0789$ Å, with transverse-energy eigenvalues for beam energies of (a) $\gamma = 35.35$, (b) $\gamma = 41.07$, (c) $\gamma = 61.15$, and (d) $\gamma = 106.76$.